Acidic properties of sulfonic acid-functionalized FSM-16 mesoporous silica and its catalytic efficiency for acetalization of carbonyl compounds

Ken-ichi Shimizu [a],[*],[1], Eidai Hayashi [a], Tsuyoshi Hatamachi [b], Tatsuya Kodama [b],
Tomoya Higuchi [c], Atsushi Satsuma [c], Yoshie Kitayama [b]

[a] *Graduate School of Science and Technology, Niigata University, Ikarashi-2, Niigata 950-2181, Japan*
[b] *Department of Chemistry & Chemical Engineering, Faculty of Engineering, Niigata University, Ikarashi-2, Niigata 950-2181, Japan*
[c] *Department of Applied Chemistry, Graduate School of Engineering, Nagoya University, Chikusa-ku, Nagoya 464-8603, Japan*

Received 18 November 2004; revised 4 January 2005; accepted 16 January 2005

Abstract

Propyl-sulfonic acid-functionalized FSM-16 mesoporous silica (SO_3H-FSM) is prepared by a conventional post-modification method. For the acetalization of carbonyl compounds with ethylene glycol, SO_3H-FSM shows a higher rate and 1,3-dioxolane yield than conventional heterogeneous solid acids such as zeolites, montmorillonite K10 clay, silica-alumina, and the sulfonic resin. SO_3H-FSM is stable during the reaction, with no leaching and deactivation of sulfonic acid groups, and is reusable without loss of its activity. The acidity and hydrophilicity of SO_3H-FSM are well characterized by the microcalorimetry of NH_3 adsorption, NH_3-TPD, and H_2O-TPD, and the result is compared with those for various aluminosilicate zeolites (HZSM5, HBEA, HY) and K10 clay. It is found that NH_3-TPD is not suitable for characterizing the acidity of SO_3H-FSM, because the decomposition of SO_3H groups on SO_3H-FSM begins above 200 °C. An NH_3 adsorption microcalorimetric experiment at 150 °C shows that, compared with HZSM5, SO_3H-FSM has a smaller number of acid sites but has a similar number of strong acid sites with ammonia adsorption heat above 140 kJ mol^{-1}. Comparison of the structural properties and catalytic results shows that a large pore diameter and low hydrophilicity are required to obtain high activity. Brønsted acid sites with a relatively strong acid strength are more suitable for this reaction, but the high acid concentration is not indispensable. The high activity of SO_3H-FSM should be caused by the presence of the strong Brønsted acid sites in the mesopore with a relatively low hydrophilicity, where both reactants can smoothly access the acid sites.

© 2005 Elsevier Inc. All rights reserved.

Keywords: Acetalization; Mesoporous silica; Sulfonic acid; TPD; Microcalorimetry

1. Introduction

Aldehydes and ketones are frequently protected as acetals in the course of organic synthesis [1]. 1,3-Dioxolane is one of the most popular protecting groups for this purpose. Although synthesis of 1,3-dioxolane is generally performed with the use of ethylene glycol in the presence of homogeneous acid catalysts such as *p*-toluenesulfonic acid (PTSA) and pyridinium salts [2–5], these homogeneous catalysts present limitations due to the use of toxic and corrosive reagents, the tedious workup procedure, and the necessity of neutralization of the strong acid media, producing undesired wastes. To overcome these problems, various heterogeneous catalysts such as zeolites [6–8], functionalized zeolite [9], Ti-exchanged clay [10], and alumina [11] have been employed for the synthesis of 1,3-dioxolane from carbonyl compounds and ethylene glycol. However, some of these procedures suffer because of a high catalyst/substrate ratio and a long reaction time. For zeolites, the microporous structure can limit the accessibility of substances to the internal acid sites [9], the products or by-products can be strongly

adsorbed to the strong acid sites present in the micropore, and thus, before catalyst reuse, a regeneration of the zeolite by high-temperature calcination is required to remove adsorbed species [8].

The use of organically functionalized mesoporous silica as a catalyst for organic synthesis has received considerable attention [12–27]. Among these materials, sulfonic acid-functionalized mesoporous silicas can be alternatives to commercially available sulfonic resins, which suffer from low surface area and thermal stability. Although the catalytic applications of the resins for organic synthesis have been well established [28,29], relatively few examples of the use of sulfonic acid mesoporous silica for organic reactions have been reported [16–24]. For a fundamental understanding of this new class of the solid acid, it is informative to clarify the structural characteristics, such as the numbers and strength of acid sites and hydrophilicity in comparison with conventional solid acid catalysts and to reveal the effect of these factors on the catalytic activity. However, little attention has been focused on this aspect. As a part of ongoing research on the catalysis of functionalized silicas for clean organic synthesis [25–27,30], we present here sulfonic acid-functionalized FSM-16 mesoporous silica (SO₃H-FSM) as a highly effective and reusable catalyst for the acetalization of various carbonyl compounds with ethylene glycol. Detailed characterizations show the number and strength of acid sites and the hydrophilicity of SO₃H-FSM in comparison with conventional microporous or mesoporous solid acid catalysts. The results are discussed to reveal the factors affecting the catalytic activity for the acetalization reaction.

2. Experimental

2.1. Catalyst preparation and characterization

FSM-16 silica was prepared from kanemite according to a method previously described [31]. Sulfonic acid-functionalized FSM-16 mesoporous silica (SO₃H-FSM) was prepared as follows. The FSM-16 sample (2 g) was dried at $120\,^{\circ}\mathrm{C}$, and then 3-mercaptopropyltriethoxysilane (2 mmol) in dry toluene (20 ml) was introduced. The mixture was refluxed for 6 h, and the solid was filtered off, washed with toluene and acetone, and air-dried. The SH groups were converted into SO_3H groups by oxidation in a mixture of aqueous H_2O_2 (31%, 5 ml) and CH_3CN (30 ml) for 6 h at a reflux temperature. After filtration and washing with water and ethanol, the sample was then acidified in 0.1 M H_2SO_4 solution for 1 h, followed by washing with water until neutral pH and drying at $100\,^{\circ}\mathrm{C}$ for 6 h.

Montmorillonite K10 clay (surface area (S_{BET}) = $220\ \mathrm{m^2\,g^{-1}}$) and a sulfonic resin (Amberlyst-15; S_{BET} = $45\ \mathrm{m^2\,g^{-1}}$) were purchased from Aldrich. To remove residual metal cations in the cation-exchange site in the clay, K10 clay (1 g) was treated in an aqueous solution of NH_4NO_3 (1 M, 10 ml) at room temperature for 3 h, fol-

lowed by calcination at $500\,^{\circ}\mathrm{C}$ for 1 h. Amorphous silica (JRC-SIO-8, a reference catalyst of the Catalysis Society of Japan; $S_{BET} = 303\ \mathrm{m^2\,g^{-1}}$), silica-alumina (JRC-SAL-2, $SiO_2/Al_2O_3 = 5.6$, $S_{BET} = 560\ \mathrm{m^2\,g^{-1}}$), HY zeolite (JRC-Z-HY4.8, $SiO_2/Al_2O_3 = 4.8$, $S_{BET} = 663\ \mathrm{m^2\,g^{-1}}$), HZSM5 zeolite (JRC-Z5-25H, $SiO_2/Al_2O_3 = 25$), and HBEA zeolite (JRC-Z-HB25, $SiO_2/Al_2O_3 = 25 \pm 5$) were supplied by the Catalysis Society of Japan. We prepared octadecyltriethoxysilane-treated HY zeolite (OD-HY) by refluxing a mixture of the HY zeolite (2 g) dried at $120\,^{\circ}\mathrm{C}$ and octadecyltriethoxysilane (2 mmol) in dry toluene (20 ml) for 6 h, followed by filtering and washing with toluene and acetone, and by drying at $100\,^{\circ}\mathrm{C}$ for 1 h [32]. The number of the octadecyl groups determined by the elemental analysis was $0.4\ \mathrm{mmol\,g^{-1}}$.

Sulfur content in the SO₃H-FSM was analyzed with a CS analyzer. The titration technique was used to determine the number of H^+ on the SO₃H-FSM. About 0.05 g of the sample was added to 15 ml of the 2 M NaCl solution and allowed to equilibrate. Then the liquid phase was titrated by the dropwise addition of 0.01 M NaOH(aq) [22]. XRD patterns were taken with a MX Labo (MAC Science) with Cu-K_α radiation. We obtained the BET surface area and pore size distribution by measuring N_2 adsorption isotherms at 77 K, using TriStar 3000 (Micromeritics). The pore size distribution curve was calculated by the BJH method from adsorption isotherms.

FTIR measurement of adsorbed ammonia on SO₃H-FSM was performed with a JASCO FT/IR-300. The sample was pressed into 0.03 g of self-supporting wafers and mounted in a quartz IR cell with CaF_2 windows. After evacuation of the sample at $150\,^{\circ}\mathrm{C}$ for 1 h, followed by ammonia adsorption (10 Torr) and by evacuation at $150\,^{\circ}\mathrm{C}$ for 0.5 h, a difference spectrum was recorded at room temperature.

A temperature-programmed desorption (TPD) experiment with NH_3 or H_2O was carried out with TPD equipment (BEL Japan). To the sample (0.05 g), preheated under vacuum at $150\,^{\circ}\mathrm{C}$ for 1 h, NH_3 (100 Torr) was introduced at $100\,^{\circ}\mathrm{C}$, followed by purging with He at $100\,^{\circ}\mathrm{C}$ for 0.5 h. NH_3-TPD was then carried out under He flow (60 ml min⁻¹) at a reduced pressure (200 Torr) from 100 to $650\,^{\circ}\mathrm{C}$ at a heating rate of $10\,^{\circ}\mathrm{C\,min^{-1}}$, and outlet gases were analyzed with a mass spectrometer. Although the molecular weight of NH_3 is 17, the fragment with $m/e = 16$ was used to quantify NH_3, because fragment 17 is affected by the desorbed water [33,34]. For H_2O-TPD, H_2O (20 Torr) was introduced into the sample (0.05 g) at $25\,^{\circ}\mathrm{C}$, followed by purging with He at $50\,^{\circ}\mathrm{C}$ for 1 h; we performed TPD in He flow (60 cm³ min⁻¹) at a reduced pressure (200 Torr) by raising the temperature from 50 to $650\,^{\circ}\mathrm{C}$ at a rate of $10\,^{\circ}\mathrm{C\,min^{-1}}$, and outlet gases ($m/e = 18$) were analyzed with a mass spectrometer.

Microcalorimetric measurement of NH_3 adsorption was performed at $150\,^{\circ}\mathrm{C}$ with a calorimeter (Tokyo Rikou Co., HAC-450G) connected to a volumetric glass line ($35\,^{\circ}\mathrm{C}$) with on-line injection system for pulsing NH_3 gas. Before

the adsorption experiments the sample (0.1 g) was pretreated under vacuum overnight at 150 °C (for SO$_3$H-FSM and K10 clay) or 400 °C (for HZSM5), respectively.

2.2. Catalytic test

Toluene was dried over 3A sieves. Ethylene glycol and carbonyl compounds were obtained from commercial sources and were used without further purification. Typically, we performed acetalization simply by refluxing the mixture of carbonyl compound (5 mmol) and ethylene glycol (6 mmol) in toluene (5 ml) in air. Under these conditions, a part of the water produced can remain in the reaction media, and some water can move to the condenser after the azeotropic removal of water. For the reaction with SO$_3$H-FSM catalyst, the catalyst amount was 7 mg, corresponding to 0.1 mol% with respect to carbonyl compounds (0.001 mol of SO$_3$H groups/mol of carbonyl compounds). For the kinetic test in Fig. 5, the catalyst amount was 7 mg for SO$_3$H-FSM, FSM-16 silica, 10 mg for Amberlyst-15, and 30 mg for other catalysts. Yields were determined by GC with n-dodecane as an internal standard. The products were identified by ^{1}H NMR. We measured the reproducibility of the catalytic test by repeating it three times for the acetalization of acetophenone (5 mmol) with ethylene glycol (6 mmol) in toluene (5 ml) at reflux temperature by SO$_3$H-FSM (7 mg). The relative error was estimated to be 6%.

3. Results and discussion

3.1. Characterization

The XRD pattern of SO$_3$H-FSM showed a typical low-angle reflection (100) at $d_{100} = 3.65$ nm characteristic of FSM-16 [31], indicating that the long-range ordered structure of the support was preserved. Fig. 1 shows pore size distribution curves for SO$_3$H-FSM and FSM-16. Clearly, introduction of R–SO$_3$H groups resulted in a smaller pore diameter and a broader distribution curve. For FSM-16, surface area (951 m^2 g^{-1}), pore volume (1.2 cm^3 g^{-1}), and pore diameter (around 2.6 nm) were as expected for mesoporous materials. These values were reduced after the introduction of R–SO$_3$H groups (surface area = 858 cm^3 g^{-1}, pore volume = 0.90 cm^3 g^{-1}, pore diameter = 2.3 nm), which could be due to the presence of R–SO$_3$H groups in the channels of FSM-16.

The sulfur content of SO$_3$H-FSM was 0.77 mmol g^{-1}. The number of H$^+$ determined by acid-base titration was 0.77 ± 0.02 mmol g^{-1}. This value is very close to the sulfur content, indicating that most of the sulfur species on the sample are in the form of the sulfonic acid groups without forming disulfides [17]. Note that the amount of H$^+$ for unmodified FSM-16 silica was below the detection limit of the titration, confirming that the acidity of SO$_3$H-FSM is caused
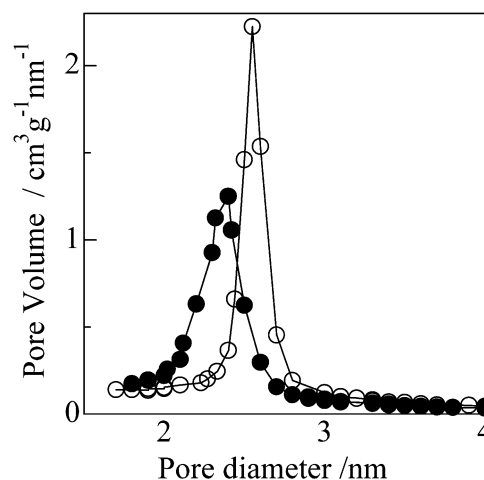

Fig. 1. The pore size distribution curves of SO$_3$H-FSM (●) and FSM-16 (○).

by the sulfonic groups. The type of acid sites in SO$_3$H-FSM was first confirmed by FTIR measurement of adsorbed NH$_3$ (result not shown). The spectrum of adsorbed NH$_3$ on SO$_3$H-FSM showed N–H vibration (in the range of 3000–3300 cm^{-1}) and deformation (1420 cm^{-1}) bands of NH$_4$$^+$ ion accompanying expanses of the bands due to acidic hydroxyl groups in a range of 3600–3700 cm^{-1} and the asymmetric stretching band of SO$_2$ moieties at 1370 cm^{-1}. This indicates that NH$_4$$^+$ ions are formed by the interaction of NH$_3$ with Brønsted acid sites in SO$_3$H groups.

Fig. 2 shows the NH$_3$-TPD curve for SO$_3$H-FSM. A large desorption peak centered around 170 °C was observed. Note that no desorption peak appeared in the NH$_3$-TPD curve of the unmodified FSM-16 silica, which confirms that the peak for SO$_3$H-FSM is assigned to the NH$_3$ desorption from SO$_3$H groups. The desorption peaks are clearly smaller for SO$_3$H-FSM than those for zeolites, indicating a smaller acid amount of SO$_3$H-FSM. The number of NH$_3$ desorbed from each sample in the range of 100 to 650 °C is listed in Table 1. The number of NH$_3$ desorbed from SO$_3$H-FSM was 0.43 mmol g^{-1}. The desorption temperature for SO$_3$H-FSM was lower than those for zeolites (HY, HBEA, and HZSM5), which may suggest a weaker acid strength for SO$_3$H-FSM compared with zeolites. However, at a temperature range of 200–600 °C, a SO$_2$ ($m/e = 64$) desorption peak (a dotted line in Fig. 1) was also observed, which indicates the decomposition of SO$_3$H groups on this sample above 200 °C. Hence, NH$_3$-TPD is not an appropriate method for characterizing the acidity of SO$_3$H-FSM. The NH$_3$-TPD curve of octadecyltriethoxysilane-treated HY zeolite (OD-HY) is also included in Fig. 1. The number of desorbed NH$_3$ from HY did not significantly decrease after the introduction of octadecyl groups. Thus, the silanol groups, mainly present at the external surface of the zeolite, may be preferably consumed by the reaction with octadecyltriethoxysilane.

Because the decomposition of SO$_3$H groups on SO$_3$H-FSM begins above 200 °C, we performed an NH$_3$ adsorption microcalorimetric experiment at 150 °C to obtain more
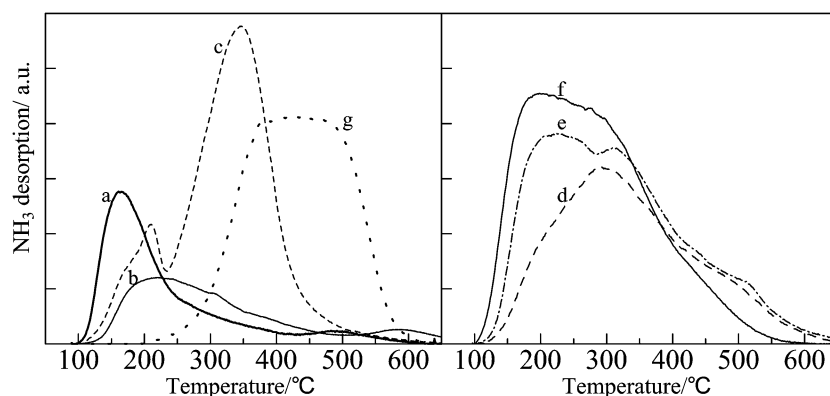
Fig. 2. NH$_3$-TPD curves ($m/e = 16$) for (a) SO$_3$H-FSM, (b) K10 clay, (c) HZSM5, (d) HBEA, (e) OD-HY and (f) HY. A dotted line (g) denotes the MS signal intensity curves for $m/e = 64$ (SO$_2$) during the NH$_3$-TPD experiment of SO$_3$H-FSM.

Table 1
Summary of the acetalization results[a] and structural characteristics of the catalysts

Catalysts	Rate[b] (mmol h^{-1} g^{-1})	Yield[c] (%)	Q_{NH_3}[d] (kJ mol^{-1})	N_{100}[e] (mmol g^{-1})	N_{130}[f] (mmol g^{-1})	N_{NH_3}(TPD)[g] (mmol g^{-1})	N_{H_2O}(TPD)[h] (mmol g^{-1})	Pore diameter (nm)
SO$_3$H-FSM	505	91	175	0.33	0.08	0.43	0.27	2.3 nm[i]
HBEA	60	47	–	–	–	1.04	0.32	0.76 nm × 0.64 nm[j]
OD-HY	58	45	–	–	–	1.40	1.04	(0.74 nm)[k]
K10 clay	14	54	131	0.10	0	0.37	0.07	2.5 nm[i]
HY	5	19	–	–	–	1.43	1.29	0.74 nm[j]
HZSM5	4	13	187	1.00	0.10	1.17	0.16	0.53 nm × 0.56 nm[j]

[a] Results in Fig. 5.
[b] Initial rate of acetal formation.
[c] GC yields after 10 h.
[d] The initial adsorption heat of chemisorbed NH$_3$ in NH$_3$ microcalorimetry.
[e] The number of chemisorbed NH$_3$ having heats of adsorption above 100 kJ mol^{-1} in NH$_3$ microcalorimetry.
[f] The number of chemisorbed NH$_3$ having heats of adsorption above 140 kJ mol^{-1} in NH$_3$ microcalorimetry.
[g] The number of desorbed NH$_3$ in a range 100–650 °C in NH$_3$-TPD.
[h] The number of desorbed H$_2$O in a range 50–200 °C in H$_2$O-TPD.
[i] Pore diameters estimated by N$_2$ adsorption using the BJH equation.
[j] Pore diameters from crystallographic data.
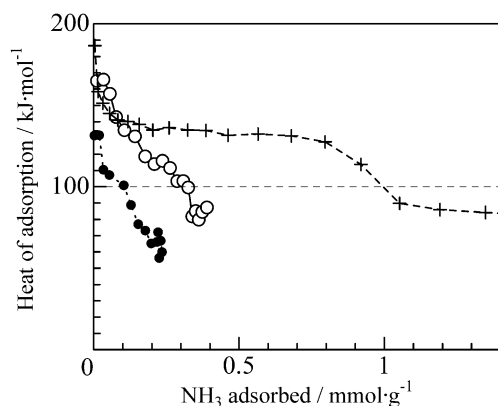[k] The pore diameter of the unmodified HY.

Fig. 3. Differential heat of adsorption of NH$_3$ on (○) SO$_3$H-FSM, (●) K10 clay and (+) HZSM5.

reliable information on the acidity (number and strength of acid sites) of this catalyst. Fig. 3 compares the curves of the differential heat of ammonia adsorption on SO$_3$H-FSM, K10 clay, and a typical zeolite, HZSM5. It is es-

tablished that NH$_3$ adsorption on Brønsted acid sites on several H$^+$-exchanged zeolites produced heats in the range of 100–150 kJ mol^{-1} [35–37]. Similar to the published results [35–37], HZSM5 shows an initial heat of adsorption of 183 kJ mol^{-1}, a plateau of very similar differential heat between 130 and 150 kJ mol^{-1}, and a sharp drop in the heat above the surface coverage of around 1.0 mmol g^{-1}. This feature indicates that the majority of Brønsted acid sites in HZSM5 are homogeneous in terms of the acid strength, which is in good agreement with a quite narrow feature of the NH$_3$-TPD curve for HZSM5 (Fig. 2). SO$_3$H-FSM exhibits an initial heat of approximately 175 kJ mol^{-1}. The heat of adsorption gradually decreases with an increase in the amounts of adsorbed NH$_3$, steeply decreases from 100 to ca. 85 kJ mol^{-1} above the surface coverage of 0.33 mmol g^{-1}, and then shows a constant value of around 85 kJ mol^{-1}. The amounts of chemisorbed NH$_3$ can be determined from the curve. From the above-mentioned facts, we assigned the adsorption with the heat above 100 kJ mol^{-1} to the chemisorption of NH$_3$ on Brønsted acid sites and that
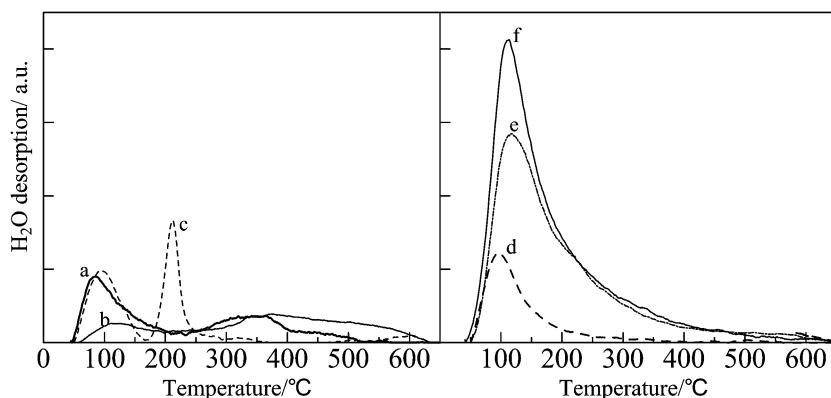
Fig. 4. H_2O-TPD curves ($m/e = 18$) for (a) SO_3H-FSM, (b) K10 clay, (c) HZSM5, (d) HBEA, (e) OD-HY and (f) HY.

with the heat below 100 kJ mol^{-1} to weak adsorption, possibly via hydrogen bonding, on the site that should not be catalytically relevant. As listed in Table 1, the number of chemisorbed NH_3 on Brønsted acid sites of SO_3H-FSM and HZSM5 are 0.33 mmol g^{-1} and 1.0 mmol g^{-1}, respectively, indicating the smaller number of Brønsted acid sites in SO_3H-FSM than that in HZSM5. However, the number of acid sites with the heat above 140 kJ mol^{-1} for SO_3H-FSM (0.08 mmol g^{-1}) and HZSM5 (0.10 mmol g^{-1}) are close to each other, indicating that the number of strong acid sites in SO_3H-FSM is close to that in a typical aluminosilicate zeolite, HZSM5. The strength of the acid sites of SO_3H-FSM is heterogeneous: with increasing volume of adsorbed ammonia, the adsorption heat decreases continuously. The number of Brønsted acid sites in SO_3H-FSM determined by the microcalorimetric experiment (0.33 mmol g^{-1}) is lower than the number of H$^+$ determined by acid-base titration (0.77 ± 0.02 meq g^{-1}) and the sulfur content (0.77 mmol g^{-1}). The reason for these results is not clear, but we believe that interaction between a SO_3H group and neighboring SO_3H groups or SiOH groups on the support is responsible for the heterogeneous distribution of the acid strength of SO_3H-FSM. Fig. 3 includes the curves of the differential heat for K10 clay. K10 clay exhibits an initial heat of 131 kJ mol^{-1}, and the heat of adsorption decreases with an increase in the amounts of adsorbed NH_3. The number of acid sites with the heat above 100 kJ mol^{-1} is 0.10 mmol g^{-1}. This indicates that the number and the strength of acid sites in K10 clay are smaller than those for HZSM5 and SO_3H-FSM.

To compare the hydrophilicity of the samples, H_2O-TPD was carried out. As shown in Fig. 4, a desorption peak centered around 80–120 °C is observed for all of the samples. For SO_3H-FSM, a SO_2 desorption peak ($m/e = 64$, result not shown) was observed in the temperature range of 200–600 °C, indicating a thermal decomposition of SO_3H groups. A H_2O desorption peak in the range of 200–600 °C should be caused by the thermal decomposition of SO_3H groups and by the dehydration of surface Si–OH groups on SO_3H-FSM. The decomposition temperature of SO_3H groups (200 °C) is lower than the reaction temperature for typical liquid-phase organic reactions catalyzed by acid cat-

alysts, and hence SO_3H-FSM can be stable during most of the reaction. In this study we assumed that H_2O desorption below 200 °C mainly originates from the physisorbed H_2O, and the number of H_2O desorbed from various samples in a temperature range of 50–200 °C (Table 1) is used to compare the hydrophilicity of different samples. It is reasonable to assume that the sample with a higher number of desorbed H_2O shows higher hydrophilicity. The hydrophilicity of the samples changed in the order of K10 clay < HZSM5 < SO_3H-FSM < HBEA < OD-HY < HY.

3.2. Structure-activity relationship for acetalization

The solid acids characterized in the above section were tested in the acetalization of acetophenone with ethylene glycol by refluxing in air (Fig. 5). From the slope of this kinetic plot, the initial rate per gram of the catalyst was estimated. The rate changed in the order of SO_3H-FSM > Amberlyst-15 > HBEA = OD-HY > FSM-16 > HY > HZSM5 > silica-alumina = amorphous silica. Tanaka et al. [38] reported that siliceous mesoporous material (MCM-41) catalyzed the acetalization of carbonyl compounds by methanol. We have found that the mesoporous silica, FSM-16, also catalyzes the acetalization of acetophenone by ethylene glycol without loading of SO_3H. However, the initial rate per gram of the catalyst was 15 times higher for SO_3H-FSM than for FSM-16, and, hence, the anchored SO_3H group is the main catalytic species of SO_3H-FSM. Under the present conditions, SO_3H-FSM was more effective than conventional solid acids such as silica-alumina, H$^+$-exchanged zeolites (HBEA, HY, and HZSM5), montmorillonite K10 clay, and a sulfonic resin (Amberlyst-15). Taking into account the acid amount of Amberlyst-15 (4.8 mmol g^{-1}) [22], the rate per acid site for SO_3H-FSM (656 h^{-1}) is estimated to be 9 times higher than that for the resin (70 h^{-1}). The lower rate of Amberlyst-15 could be related to the low accessibility of the reactant to the acid sites inside the bulk of Amberlyst-15, which has a relatively low surface area (45 m^2 g^{-1}).

A comparison of the catalytic results for microporous or mesoporous solid acid and structural characteristics are shown in Table 1. The result shows that low hydrophilic-
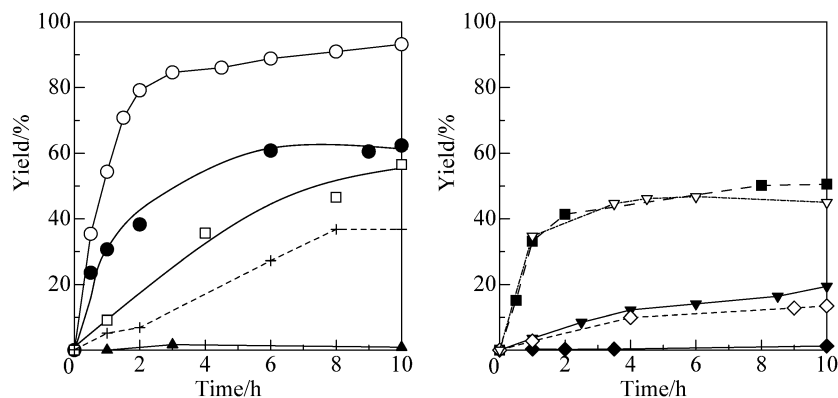
Fig. 5. Plot of GC yield versus time for the acetalization of acetophenone (5 mmol) with ethylene glycol (6 mmol) in toluene (5 ml) at reflux temperature by various catalysts: (○) SO$_3$H-FSM, (●) Amberlyst-15, (□) K10 clay, (+) FSM-16 silica, (▲) amorphous silica, (◆) silica-alumina, (▼) HY, (◇) HZSM5, (■) HBEA, and (▽) OD-HY. Catalyst amount was 7 mg for SO$_3$H-FSM, FSM-16 silica, 10 mg for Amberlyst-15, and 30 mg for other catalysts.

ity and large pore diameter are primarily important factors as described below. Ogawa et al. [32] reported that highly hydrophobic zeolite was prepared by octadecyltrichlorosilane treatment of HZSM5. To investigate the effect of hydrophobicity of the catalyst on the activity, we prepared octadecyltriethoxysilane-treated H-Y zeolite (OD-HY) and used it for the acetalization of acetophenone. It is noteworthy that the initial rate of product formation and the final yield of HY zeolite were greatly enhanced by the modification with the octadecyl groups, and the result could be explained as follows. In the absence of octadecyl groups, the HY zeolite with a low SiO$_2$/Al$_2$O$_3$ ratio (4.8) is highly hydrophilic, as indicated by H$_2$O-TPD. Hence polar molecules, such as ethylene glycol and water produced by the reaction, should be strongly adsorbed on the acid site, resulting in blocking of the site. As a result of a decrease in the hydrophilicity with the introduction of octadecyl groups, a less polar substance, acetophenone, can be more accessible to the acid site in HY, and thus the activity is improved. The importance of the hydrophobicity of zeolite for the acetalization by ethylene glycol was demonstrated by Climent et al., who observed a relatively low activity of the Al-rich zeolites [8]. HZSM5, with relatively low hydrophilicity, shows the lowest activity. This can be explained by the small pore diameter of this sample. The retarding effect of geometrical constraints on the catalytic activity of zeolites was clearly illustrated by Climent et al. for the dimethylacetal formation in the study of the influence of the zeolite crystal size on the reaction rate [39]. The geometrical constraints could inhibit diffusion of the reactant and the bulkier reaction products in the pore of HZSM5, which has the smallest pore size among the catalysts tested in our study. Among the unmodified zeolites, HBEA shows the highest rate, possibly because the catalyst has both a large pore diameter (0.76 nm × 0.64 nm) and a relatively low hydrophilicity. Taking into account the fact that SO$_3$H-FSM also has hydrophobic groups (CH$_2$ groups) and hence the catalyst shows a relatively low hydrophilicity (Table 1), it is suggested that the higher activity of SO$_3$H-FSM compared with zeolites is partly due to its hydrophobic nature and its larger-diameter channels. We checked the effect

of water removal during the reaction by 0.5 g of molecular sieves (MS4A) placed in the condenser, with HBEA as a catalyst (not shown). The yield after 10 h of the reaction was 71%, and the yield did not increase after 24 h. This value is higher than the yield with HBEA under standard conditions (47%), where a part of the water produced during the reaction can remain in the reaction media. This indicates that a shift of the equilibrium with the removal of water from the reaction media is effective in obtaining a high yield. However, a moderate yield under dry conditions (71%) suggests that the activity is also retarded by other effects, such as strong poisoning of water on acid sites in the micropore.
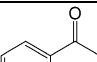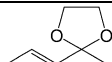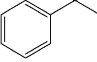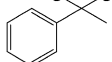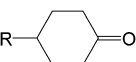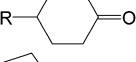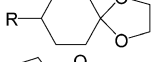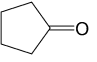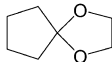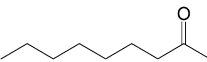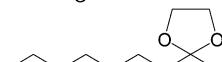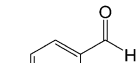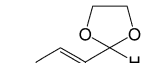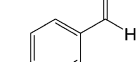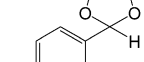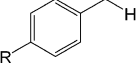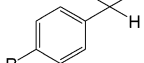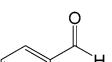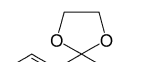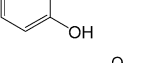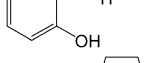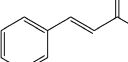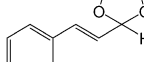
Comparison of the number of acid sites with the reaction rates (Table 1) clearly indicates that a large number of acid sites per gram of the catalyst is not necessarily required for 1,3-dioxolane formation; HY and HZSM5, with a relatively large number of acid sites, show a lower rate than K10 clay and SO$_3$H-FSM, with a smaller number of acid sites. Although K10 clay exhibits low hydrophilicity and a large pore diameter, it shows much lower activity than SO$_3$H-FSM. The higher acid strength of SO$_3$H-FSM than K10 clay, as shown by microcalorimetric experiment, should be responsible for the higher activity of SO$_3$H-FSM.

From the above discussion, the factors affecting the acetalization of the carbonyl compound with ethylene glycol are summarized as follows. Large pore diameter and low hydrophilicity are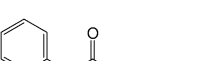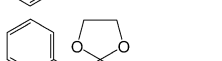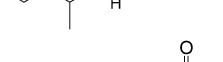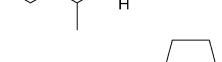 required to obtain a high reaction rate and a high yield of the 1,3-dioxolane. Brønsted acid sites with a relatively strong acid strength are suitable for this reaction, but the high acid concentration is not necessarily required. The high activity of SO$_3$H-FSM should be caused by the low hydrophilicity of the strong Brønsted acid sites present in the mesopore, where both reactants can smoothly access to the acid sites.

3.3. Catalytic performance of SO$_3$H-FSM for acetalization

As shown in Fig. 5, SO$_3$H-FSM (0.1 mol%) effectively catalyzed the acetalization of acetophenone with ethylene glycol. No measurable by-products were observed by TLC,

Table 2
SO$_3$H-FSM catalyzed acetalization of carbonyl compounds with ethylene glycol[a]

Entry	Substrate	Time	Product		Conversion[b] (%)	Yield[c] (%)
1	(acetophenone)	10	(product)	R = H	96	93
2						
3	(4-R-cyclohexanone)	3	(product)	R = H	99	90
4		1		R = Bu^t	98	89
5	(cyclopentanone)	3	(product)		99	88
6	(2-nonanone)	3	(product)		91	91
7	(4-R-benzaldehyde)	1	(product)	R = H	99	90
8		1		R = Cl	98	94
9		12		R = OCH$_3$	97	80
10	(salicylaldehyde)	12	(product)		77	74
11	(cinnamaldehyde)	8	(product)		84	81
12	(2-phenylpropanal)	2	(product)		99	99
13	(n-octanal)	3	(product)		99, 98[d], 99[e], 98[f]	99, 97[d], 98[e], 96[f]
14	(citronellal)	1	(product)		93	88

[a] The reaction was performed by simply refluxing the mixture of carbonyl compound (5 mmol) and ethylene glycol (6 mmol) in toluene (5 ml) with a catalyst (0.1 mol%, 7 mg) in air.

[b] Conversions of carbonyl compounds determined by GC using internal standard method.

[c] Yields of acetals determined by GC.

[d] Second cycle.

[e] Third cycle.

[f] Fourth cycle.

GC, or ^{1}H NMR analyses. After the reaction, SO$_3$H-FSM was removed by centrifugation and was washed with acetone, followed by drying at 100 °C for 1 h. The titration experiment of the recovered catalyst showed that the number of acid sites (0.77 ± 0.01 meq g^{-1}) did not change after the reaction, which indicates that no leaching or deactivation of sulfonic acid groups occurred during the reaction. A possible contribution of homogeneous catalysis was excluded in the following experiment. When the SO$_3$H-FSM was removed at an early stage of the reaction ($t = 10$ min, 20% yield), the reaction did not proceed further, confirming that the observed catalysis of SO$_3$H-FSM is truly heterogeneous in nature. After the first run, the reusability of the SO$_3$H-FSM was tested. For the acetalization of *n*-octanal, the catalyst can be recycled at least three times while keeping almost quantitative conversion without any reactivation treatment (entry 13 in Table 2).

As summarized in Table 2, the present method was widely applicable for 1,3-dioxolane synthesis from various ketones (entries 1–6) and aldehydes (entries 7–14) with good yields (90–98%), by simply refluxing for 1–12 h. Aromatic aldehydes, aliphatic aldehydes, and conjugated aldehyde underwent smooth transformation to the corresponding acetal in good yield. Cyclic, aliphatic, and aromatic ketones reacted smoothly to give the corresponding acetals. Note that sizes of the reagents and products listed in Table 2 are smaller than the mean pore diameters of the SO$_3$H-FSM catalyst (2.3 nm).

References

[1] T.W. Greene, P.G.M. Wuts, Protecting Groups in Organic Synthesis, second ed., Wiley, New York, 1991.

[2] R.A. Daignault, E.L. Eliel, Organic Synthesis, Wiley, New York, 1973.

[3] L.F. Fieser, R. Stevenson, J. Am. Chem. Soc. 76 (1954) 1728.

[4] W.G. Dauben, J.M. Gerdes, G.C. Look, J. Org. Chem. 51 (1986) 4964.

[5] N.M. Leonard, M.C. Oswald, D.A. Freiberg, B.A. Nattier, R.C. Smith, R.S. Mohan, J. Org. Chem. 67 (2002) 5202.

[6] A. Corma, M.J. Climent, H. Garcia, J. Primo, Appl. Catal. 58 (1990) 333.

[7] R. Ballini, G. Boscica, B. Frullanti, R. Maggi, G. Sartori, F. Schroer, Tetrahedron Lett. 39 (1998) 1615.

[8] M.J. Climent, A. Corma, A. Velty, M. Susarte, J. Catal. 196 (2000) 345.

[9] C.W. Jones, K. Tsuji, M.E. Davis, Nature 393 (1998) 52.

[10] T. Kawabata, T. Mizugaki, K. Ebitani, K. Kaneda, Tetrahedron Lett. 42 (2001) 8329.

[11] Y. Kamitori, M. Hojo, R. Masuda, T. Yoshida, Tetrahedron Lett. 26 (1985) 4767.

[12] J.H. Clark, D.J. Macquarrie, Chem. Commun. (1998) 853.

[13] A.P. Wight, M.E. Davis, Chem. Rev. 102 (2002) 3589.

[14] R.D. Badley, W.T. Ford, J. Org. Chem. 54 (1989) 5437.

[15] W.M. Van Rhijn, D.E. De Vos, B.F. Sels, W.D. Bossaert, P.A. Jacobs, Chem. Commun. (1998) 317.

[16] D. M Margolese, J.A. Melero, S.C. Christiansen, B.F. Chmelka, G.D. Stucky, Chem. Mater. 12 (2000) 2448.

[17] I. Diaz, C. Marquez-Alvarez, F. Mohino, J. Perez-Pariente, E. Sastre, J. Catal. 193 (2000) 283.

[18] I. Diaz, C. Marquez-Alvarez, F. Mohino, J. Perez-Pariente, E. Sastre, J. Catal. 193 (2000) 295.

[19] D. Das, J.-F. Lee, S. Cheng, Chem. Commun. (2001) 2178.

[20] K. Wilson, A.F. Lee, D.J. Macquarrie, J.H. Clark, Appl. Catal. A 228 (2002) 127.

[21] I.K. Mbaraka, D.R. Radu, V.S. Lin, B.H. Shanks, J. Catal. 219 (2003) 329.

[22] M. Chidambaram, D. Curulla-Ferre, A.P. Singh, B.G. Anderson, J. Catal. 220 (2003) 442.

[23] S. Shylesh, S. Sharma, S.P. Mirajkar, A.P. Singh, J. Mol. Catal. A 212 (2004) 219.

[24] J.A. Melero, R. van Grieken, G. Morales, V. Nuno, Catal. Commun. 5 (2004) 131.

[25] K. Shimizu, E. Hayashi, T. Inokuchi, T. Kodama, H. Hagiwara, Y. Kitayama, Tetrahedron Lett. 43 (2002) 9073.

[26] H. Hagiwara, S. Tsuji, T. Okabe, T. Hoshi, T. Suzuki, H. Suzuki, K. Shimizu, Y. Kitayama, Green Chemistry 4 (2002) 461.

[27] K. Shimizu, H. Suzuki, E. Hayashi, T. Kodama, Y. Tsuchiya, H. Hagiwara, Y. Kitayama, Chem. Commun. (2002) 1068.

[28] G.A. Olah, P.S. Iyer, G.K.S. Prakash, Synthesis (1986) 513.

[29] M.A. Harmer, Q. Sun, Appl. Catal. A 221 (2001) 45.

[30] K. Shimizu, E. Hayashi, T. Hatamachi, T. Kodama, Y. Kitayama, Tetrahedron Lett. 45 (2004) 5135.

[31] S. Inagaki, Y. Fukushima, K. Kuroda, J. Chem. Soc., Chem. Commun. (1993) 680.

[32] H. Ogawa, T. Koh, K. Taya, T. Chihara, J. Catal. 148 (1994) 493.

[33] M. Niwa, N. Katada, Catal. Surv. Jpn. 1 (1997) 215.

[34] N. Katada, M. Niwa, Catal. Surv. Asia 8 (2004) 161.

[35] N. Cardona-Martinez, J.A. Dumesic, Adv. Catal. 38 (1992) 149.

[36] A. Auroux, Top. Catal. 4 (1997) 71.

[37] V. Solinas, I. Ferino, Catal. Today 41 (1998) 179.

[38] Y. Tanaka, N. Sawamura, M. Iwamoto, Tetrahedron Lett. 39 (1998) 9457.

[39] M.J. Climent, A. Corma, S. Iborra, M.C. Navarro, J. Primolty, J. Catal. 161 (1996) 783.